International Journal of Advanced Engineering and Technology Research
ISSN: 3106-8677 (Print), ISSN: 3106-8685 (Online) | Vol. 2, No. 1, 2026

Measurement of SiC Epilayer Thickness Using Infrared Interferometry

Dongsheng Xiang *, Zijin Xia #, Yueyang Wang #

School of Information and Artificial Intelligence, Yangzhou University, Yangzhou, 225127, China

* **Corresponding author**: (Email: 19551657020@163.com)

#These authors contributed equally

Abstract: Accurate measurement of the thickness of silicon carbide (SiC) epitaxial layers is crucial for device performance. Although infrared interferometry offers the advantages of being non-destructive and highly precise, it has limitations in terms of model accuracy and data processing. To address these challenges, this paper establishes an improved measurement methodology. First, a dual-beam interference model is constructed to inversely determine the thickness by correlating interference fringes with wavelength and incident angle. Subsequently, an enhanced computational algorithm is implemented, which includes detrending of experimental spectra and the introduction of the Cauchy dispersion formula to correct for the wavelength-dependent refractive index. The thicknesses calculated based on data at incident angles of 10° and 15° are 7.39 μm and 7.33 μm, respectively, with a cross-validation relative error of only 0.82%. Further optimization using dual-angle joint fitting yields a thickness of 7.43 μm. The results demonstrate that the model exhibits good accuracy and robustness, providing a reliable non-destructive measurement method for SiC epitaxial layer characterization and contributing to quality control in semiconductor processes.

Keywords: Epitaxial Layer Thickness, Infrared Interferometry, Cauchy's Formula, Dual-angle Joint Fitting.

1. Introduction

As a representative material of the third-generation semiconductors, silicon carbide (SiC) possesses superior physical properties—including a wide bandgap, high critical breakdown electric field, and excellent thermal conductivity—making it highly promising for applications in power electronics, new energy vehicles, and 5G communication systems. In these applications, the thickness of the epitaxial layer is one of the key parameters affecting device performance and reliability. Its accurate measurement is crucial for process control and product quality assurance. Traditional destructive measurement methods, such as cross-sectional scanning electron microscopy (SEM), offer high precision but suffer from significant limitations, including sample destruction, low efficiency, and inability to perform full-wafer mapping. In contrast, infrared (IR) interferometry, as a non-destructive and non-contact optical measurement technique, offers distinct advantages such as single-measurement full-wafer coverage and nanometer-level accuracy. It has thus become the mainstream solution for epitaxial layer thickness characterization in the industry. However, in practical applications, this method still faces challenges, including systematic errors due to model simplifications, the influence of material dispersion effects, and complications arising from multiple-beam interference at interfaces. These issues limit its application in scenarios requiring higher measurement precision.

Extensive research has been conducted on SiC epitaxial layer thickness measurement using infrared interferometry. Lu et al. investigated the effect of hot-wall CVD preparation processes on the thickness uniformity of 8-inch SiC epitaxial layers, highlighting the importance of process control for achieving uniform epitaxial growth [1]. Cristiano established fundamental design considerations for high-temperature image sensors in 4H-SiC, providing essential material parameters including the Cauchy dispersion coefficients used in this study [2]. Wang et al. developed spectral interference thin-film thickness measurement technology based on a xenon light source, advancing practical measurement techniques for epitaxial layer characterization [3]. Regarding theoretical foundations, Qiu et al. analyzed the conditions for half-wave loss when light propagates from optically denser to optically thinner media, contributing to accurate phase difference calculations in interference models [4]. Ye et al. proposed a measurement method for the Verdet constant based on the Cauchy dispersion formula, demonstrating the applicability of dispersion correction in optical characterization [5]. Liu further discussed half-wave loss and thin-film interference phenomena, refining the understanding of phase changes at interfaces crucial for precise thickness determination [6].

Despite significant progress, existing methods still exhibit several limitations: (1) Most models do not adequately account for the significant dispersion of material refractive indices in the infrared spectrum, often relying on empirical constants, which introduces systematic errors in broad-spectrum measurements. (2) The integration between data preprocessing and thickness inversion algorithms is insufficient, failing to fully leverage the entire spectral information for robust estimation. (3) Quantitative analysis of multiple-beam interference effects and effective compensation methods remain underdeveloped, with a lack of systematic validation for specific material systems, such as homoepitaxial SiC. To address these shortcomings, this study aims to develop a more accurate and robust methodology for infrared interferometric measurement. Specifically, this study first establish a rigorous mathematical model for dual-beam interference, deriving the thickness expression through Snell's law and phase conditions. Second, at the algorithmic level, it integrate spectral detrending with the Cauchy dispersion formula to correct for the wavelength-dependent refractive index. It further develop two complementary approaches for thickness inversion: a fringe spacing method based on multiple extrema and a dual-angle joint objective function optimization method, enabling high-precision thickness determination and cross-validation. Finally, by analyzing experimental data from SiC epitaxial wafers, this work validates the reliability of the proposed methodology, offering an effective solution for in-line, non-destructive thickness monitoring in semiconductor manufacturing processes.

2. Model Development

2.1. Dual-Beam Interference Mode

The dual-beam interference model is a fundamental optical model established to describe the interference pattern formed by two reflected light beams from the front and rear interfaces of an epitaxial layer. Based on the assumption that only one reflection occurs at the epitaxial layer-substrate interface, this model mathematically characterizes the relationship between the epitaxial layer thickness and the resulting interference fringes. By analyzing the optical path difference and phase difference between the two reflected beams, the model provides a theoretical foundation for calculating the epitaxial layer thickness from measured interference spectra.

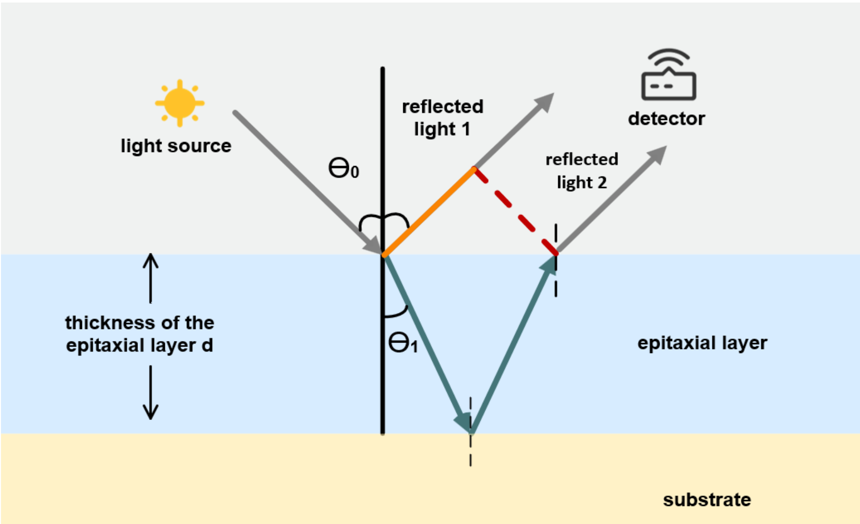

Figure 1. Schematic diagram of dual-beam interference

Figure 1 illustrates the optical path of light propagation in the epitaxial layer structure. As shown, incident light strikes the epitaxial layer surface at point A with an incident angle θ_0. Part of the light is directly reflected at the surface, forming beam AD. The remaining light refracts into the epitaxial layer at an angle θ_1, propagates to point B at the epitaxial layer-substrate interface, undergoes reflection, and exits at point C. These two reflected beams superimpose to generate interference.

The optical path difference (OPD) between the two reflected beams can be derived from geometric optical path analysis:

$$\begin{cases} OPD = n_1(\bar{AB} + \bar{BC}) - n_0\bar{AD} \\ \bar{AB} = \bar{BC} = \frac{d}{\cos\theta_1}, \bar{AD} = 2d\tan\theta_1 \sin\theta_0 \end{cases} \quad (1)$$

Where n_1 is the refractive index of the epitaxial layer, n_0 represents the refractive index of air (approximately 1), d stands for the epitaxial layer thickness, θ_0 is the incident angle, and θ_1 is the refraction angle. Solving these equations yields:

$$OPD = 2n_1 d\cos\theta_1 \quad (2)$$

When light travels from an optically less dense medium to a denser medium, the reflected light undergoes a phase change of π, equivalent to an additional half-wavelength optical path. Considering this effect, the OPD becomes:

$$OPD = \begin{cases} 2n_1 d\cos\theta_1 & n_1 \approx n_2 \\ 2n_1 d\cos\theta_1 + \frac{\lambda}{2} & n_1 < n_2 \end{cases} \quad (3)$$

Where n_2 is the refractive index of the substrate and λ refers to the wavelength of incident light.

The phase difference corresponding to the OPD is given by:

$$\delta = \frac{2\pi}{\lambda}\cdot(2n_1 d\cos\theta_1 + \phi), \qquad \phi = 0, \frac{\lambda}{2} \quad (4)$$

Where ϕ represents the additional optical path due to phase change.

Applying the interference conditions, constructive interference (bright fringes) occurs when the phase difference is an integer multiple of 2π, while destructive interference (dark fringes) occurs when it is an odd multiple of π:

$$\begin{cases} Bright\ fringes: & \delta = 2m\pi \\ Dark\ fringes: & \delta = (2m+1)\pi \end{cases} \quad (5)$$

Where m is the interference order (integer).

Combining Eq. (4) with the bright fringe condition yields the thickness formula:

$$d = \frac{(m+\epsilon)\lambda}{2n_1\cos\theta_1}, \qquad \epsilon = 0, \frac{1}{2} \quad (6)$$

Where $\epsilon = 0$ when $n_1 \approx n_2$, and $\epsilon = 1/2$ when $n_1 < n_2$.

Applying Snell's law and trigonometric identity:

$$n_0\sin\theta_0 = n_1\sin\theta_1, \sin^2\theta_1 + \cos^2\theta_1 = 1 \quad (7)$$

The final expression for epitaxial layer thickness is obtained:

$$d = \frac{(m+\epsilon)\lambda}{2\sqrt{n_1^2 - \sin^2\theta_0}} \quad (8)$$

2.2. Improved Model with Dispersion Correction and Dual-Angle Joint Fitting

Based on the dual-beam interference model, an improved computational model is developed to enhance thickness measurement accuracy by incorporating dispersion correction and multi-angle data fusion. This model addresses two key limitations of the basic model: the wavelength dependence of the refractive index and the need for robust estimation using multiple data sources.

Raw spectral data are often affected by baseline drift and low-frequency noise. To extract the periodic interference features, a detrending process is applied:

$$R_{detrend}(\tilde{\nu}) = R_{raw}(\tilde{\nu}) - R_{baseline}(\tilde{\nu}) \quad (9)$$

Where $R_{raw}(\tilde{\nu})$ is the raw reflectance at wavenumber $\tilde{\nu}$, $R_{baseline}(\tilde{\nu})$ is the baseline component, and $R_{detrend}(\tilde{\nu})$ is the detrended reflectance containing the interference oscillations.

The refractive index of semiconductor materials varies with wavelength, a phenomenon known as dispersion. The Cauchy dispersion formula describes this wavelength dependence:

$$n(\lambda) = A + \frac{B}{\lambda^2} + \frac{C}{\lambda^4} \quad (10)$$

Where $n(\lambda)$ is the wavelength-dependent refractive index, λ is the wavelength in micrometers, and A, B, and C are fitting parameters. For 4H-SiC in the infrared range, parameters $A = 2.561$ and $B = 3.4 \times 10^{-2}$ are used, with $C = 0$ as the third term contribution is negligible.

Incorporating the dispersion correction, the thickness formula becomes:

$$d = \frac{(m+\epsilon)\lambda}{2\sqrt{n^2(\lambda) - \sin^2\theta_0}} \quad (11)$$

Where $n(\lambda)$ is given by Eq. (10).

To eliminate unknown parameters m and ϵ, adjacent interference maxima are used. For two adjacent maxima at wavelengths λ_1 and λ_2:

$$\begin{cases} d = \frac{(m_1+\epsilon)\lambda_1}{2\sqrt{n^2(\lambda_1) - \sin^2\theta_0}} \\ d = \frac{(m_2+\epsilon)\lambda_2}{2\sqrt{n^2(\lambda_2) - \sin^2\theta_0}} \\ m_2 - m_1 = 1 \end{cases} \quad (12)$$

Where m_1 and m_2 are the interference orders at λ_1 and λ_2, respectively.

Solving this system yields the wavenumber difference between adjacent peaks:

$$\Delta\tilde{\nu} = \frac{1}{2d\sqrt{n^2(\lambda) - \sin^2\theta_0}} \quad (13)$$

Where $\Delta\tilde{\nu}$ is the wavenumber difference between adjacent interference maxima.

The thickness can then be calculated directly:

$$d = \frac{1}{2}\left[\frac{\sqrt{n^2(\lambda_2) - \sin^2\theta_0}}{\lambda_2} - \frac{\sqrt{n^2(\lambda_1) - \sin^2\theta_0}}{\lambda_1}\right]^{-1} \quad (14)$$

For improved accuracy, multiple adjacent peak pairs are used, and the final thickness is the arithmetic mean:

$$d_{avg} = \frac{1}{N}\sum_{i=1}^{N} d_i \quad (15)$$

Where d_i is the thickness calculated from the i-th peak pair and N is the total number of peak pairs.

To fully utilize spectral information from multiple incident angles, a reflectance model is established:

$$R(\tilde{\nu}) = R_0 + A\cos(4\pi\tilde{\nu}n(\lambda)d\cos\theta_1 + \phi_0) \quad (16)$$

Where $R(\tilde{\nu})$ is the modeled reflectance at wavenumber $\tilde{\nu}$, R_0 is the background reflectance, A is the interference amplitude, ϕ_0 is the initial phase, and θ_1 is the refraction angle satisfying Snell's law.

A joint objective function combining data from two incident angles is constructed:

$$\min S = \sum_{i=1}^{N_1}\left(R_{exp}^{(10)}(\tilde{\nu}_i) - R_{model}^{(10)}(\tilde{\nu}_i)\right)^2 + \sum_{j=1}^{N_2}\left(R_{exp}^{(15)}(\tilde{\nu}_j) - R_{model}^{(15)}(\tilde{\nu}_j)\right)^2 \quad (17)$$

Where $R_{exp}^{(10)}(\tilde{\nu}_i)$ and $R_{exp}^{(15)}(\tilde{\nu}_j)$ are experimental reflectances at 10° and 15° incidence, $R_{model}^{(10)}(\tilde{\nu}_i)$ and $R_{model}^{(15)}(\tilde{\nu}_j)$ are corresponding model predictions, and N_1, N_2 are the numbers of sampling points in the high wavenumber range for each dataset.

The nonlinear least squares method with the Levenberg-Marquardt algorithm is employed to solve this optimization problem. The workflow proceeds in two steps. First, initial fitting of each dataset separately is performed to obtain initial parameter estimates. Second, joint optimization using the combined objective function is conducted, with the average parameters from the first step as initial values, yielding the final optimized thickness d. This dual-angle approach enhances estimation robustness by simultaneously constraining the solution with independent measurements, effectively reducing systematic errors and improving measurement reliability.

3. Results and Analysis

3.1. Thickness Calculation Using Fringe Spacing Method

Following data preprocessing, the fringe spacing method based on multiple extrema was applied to calculate the epitaxial layer thickness. This method utilizes adjacent interference maxima to eliminate unknown interference order and phase offset parameters, as described by Eqs. (12) through (14) in Chapter 2.

Table 1 presents the calculated thickness values from multiple adjacent peak pairs for the 10° incidence data.

Table 1. Epitaxial layer thickness calculation using multiple extrema (Incident angle: 10°)

Angle (°)	Δv (cm⁻¹)	d (μm)
10	199.5969	7.127525
10	239.137	7.618523
10	242.987	7.497592
10	245.397	7.423960
10	261.307	6.971943
10	264.260	6.895600
10	246.362	7.394880
10	240.576	7.572732
Mean thickness d_{avg}		7.39 μm

As shown in Table 1, the individual thickness values obtained from different peak pairs range from approximately 6.90 μm to 7.62 μm, with an arithmetic mean of 7.39 μm. This result falls within the typical thickness range of 0.1-40 μm reported in previous studies for SiC epitaxial layers, providing initial validation of the measurement method.

To assess the reliability of this result through cross-validation, the same calculation method was applied to the independent dataset measured at 15° incidence. Table 2 summarizes the results.

Table 2. Epitaxial layer thickness calculation using multiple extrema (Incident angle: 15°)

Angle (°)	Δν (cm⁻¹)	d (μm)
15	197.187	7.261754
15	258.414	7.067296
15	234.309	7.794358
15	289.276	6.313438
15	229.488	7.958099
15	253.111	7.215365
15	255.040	7.160792
Mean thickness d_{avg}		7.33 μm

The mean thickness obtained from the 15° dataset is 7.33 μm. The average thickness from both datasets is 7.36 μm, and the relative error between the two independent measurements is calculated as:

$$X = \frac{|d_1 - d_2|}{d} \times 100\% = \frac{|7.39 - 7.33|}{7.36} \times 100\% \approx 0.82\% \quad (18)$$

This relative error is below 1%, indicating excellent consistency between the two independent measurements. Such close agreement demonstrates that the model possesses strong stability and reliability, and that the thickness estimation is not significantly influenced by the specific measurement angle or random errors in a single dataset.

3.2. Thickness Optimization Using Dual-Angle Joint Fitting

To further improve measurement accuracy and fully utilize the information from both datasets, the dual-angle joint objective function optimization method described by Eqs. (16) and (17) was implemented. This approach simultaneously fits the reflectance model to both experimental spectra, constraining the solution with independent measurements at different incident angles.

Figure 2 shows the optimal fitting results obtained using the Levenberg-Marquardt algorithm for nonlinear least squares optimization.

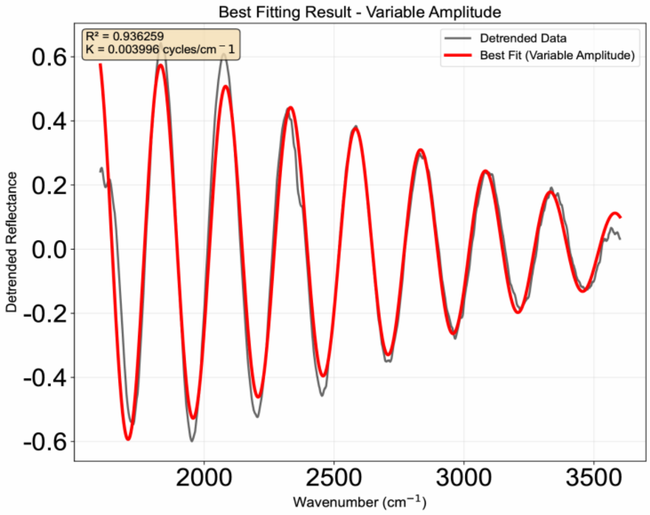

Figure 2. Optimal fitting results

As illustrated in Figure 2, the theoretical reflectance curves show excellent agreement with the experimental data for both incident angles. The model accurately reproduces the phase and amplitude characteristics of the interference fringes, particularly in the high wavenumber region where interference dominates. The goodness of fit, as indicated by the R^2 value, reaches 0.936, confirming the validity of the improved model.

Table 3 summarizes the key parameters obtained from the preliminary fitting of each dataset separately.

Table 3. Parameters after preliminary fitting

θ_0	R_0	A	φ_0	Thickness (μm)	MSE
10°	-0.00072256	0.500280837	-2.56432515	7.43198608	0.054291370
15°	0.00292512	0.501459380	2.071229317	7.43198608	0.061601855

From Table 3, it can be observed that the thickness values obtained from the preliminary fits of the 10° and 15° datasets are identical (7.43198608 μm), despite differences in other parameters such as background reflectance (R_0), amplitude (A), and initial phase (φ_0). This consistency across different incident angles further supports the reliability of the thickness estimation.

After joint optimization using both datasets simultaneously, the final optimized thickness was determined to be 7.43 μm.

4. Conclusions and Outlooks

This study establishes an improved infrared interferometry method for accurate SiC epitaxial layer thickness measurement. A dual-beam interference model was developed based on optical path analysis and Snell's law, establishing the fundamental relationship between interference fringes and layer thickness. To enhance accuracy, the model was refined by incorporating spectral detrending preprocessing and the Cauchy dispersion formula to account for the wavelength-dependent refractive index of SiC. Two complementary approaches were implemented: a multiple-extrema fringe spacing method and a dual-angle joint fitting method using nonlinear least squares optimization. Using the fringe spacing method, thickness values of 7.39 μm and 7.33 μm were obtained from independent datasets measured at 10° and 15° incidence, yielding a cross-validation relative error of only 0.82%. The dual-angle joint fitting further refined the thickness estimate to 7.43 μm, with a relative deviation of 0.95% compared to the fringe spacing results. The excellent agreement between two fundamentally different approaches confirms the reliability and robustness of the developed model. The integration of Cauchy dispersion correction eliminates systematic errors from refractive index dispersion, while the dual-angle joint fitting framework fully utilizes multi-angle measurement information, providing a reliable non-destructive measurement tool for SiC epitaxial layer characterization.

While the proposed model demonstrates strong performance, certain limitations should be acknowledged. The current model neglects physical factors such as carrier concentration effects on refractive index and non-ideal interface conditions. Future work could incorporate these factors for a more comprehensive model and extend the method to other semiconductor materials.

References

[1] Lu, R., Zheng, L., Zhang, H., et al. (2025). Effect of hot-wall CVD preparation process on thickness uniformity of 8-inch SiC epitaxial layers. Journal of Synthetic Crystals, 54(9).

[2] Cristiano, M. (2014). Design considerations for a high temperature image sensor in 4H-SiC (Doctoral dissertation). KTH Royal Institute of Technology, School of Information and Communication Technology.

[3] Wang, J., Wang, Z., Zhang, Z., et al. (2025). Research on spectral interference thin film thickness measurement technology based on xenon light source. Optical Instruments.

[4] Qiu, H., Wu, J., Xiao, D., et al. (2022). Conditions for half-wave loss when light is incident from optically denser medium to optically thinner medium. College Physics, 41(6).

[5] Ye, Y., Liang, X., & Jiang, X. (2021). Measurement method of Verdet constant based on Cauchy dispersion formula. Physics and Engineering, 31(2).

[6] Liu, J. (2024). Further discussion on half-wave loss and thin-film interference. College Physics, 43(2).